Analytic Closed Orbit Analysis for RHIC Insertion*

S.Y. Lee†
Department of Physics, Indiana University, Bloomington, IN 47405
S.Tepikian
Accel. Development Department, Brookhaven National Laboratory, Upton, NY 11973

Abstract

Analytic closed orbit analysis is performed to evaluate the tolerance of quadrupole misalignment and dipole errors (b_0, a_0) in the RHIC insertion. Sensitivity coefficients of these errors are tabulated for different β^* values. Using these sensitivity tables, we found that the power supplies ripple of 10^{-4} can cause closed orbit motion of 0.05 mm at the IP in comparison with the rms beam size of 0.3 mm. It is desirable to have the power supply ripple less than 10^{-5}.

1. Introduction

The closed orbit error in the insertion region is of fundamental important to the collider physics. For RHIC, the closed orbit at the high-β triplets may also affect the dynamical aperture. Evaluation of the sensitivity on the quadrupole alignment errors and dipole excitation or rotation angle error gives us a feeling of the alignment tolerance. Some correction schemes may also applied to obtain proper orbit control in the insertion region.

Fig. 1 shows the RHIC inserion layout. There are nine quadrupoles on both sides of the interaction point (IP). The closed orbit can result from (1) quadrupole misalignment, (2) dipole error. etc. This paper discusses an analytic method in the closed orbit analysis.

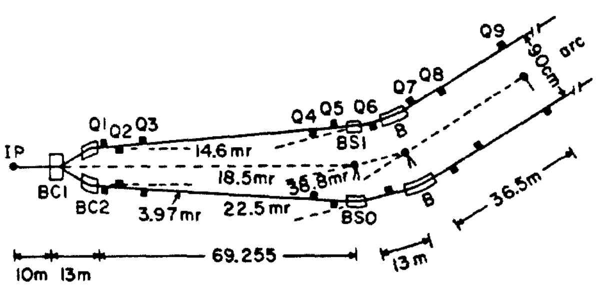

Fig. 1: Schematic Layout of a RHIC insertion.

2. Method of Orbit Error Analysis

For a particle in the accelerator, the equation of motion is given by[1]

$$\frac{d^2y}{ds^2} + K(s)y = \frac{\Delta B(s)}{B\rho} \tag{1}$$

where y represents either the radial or vertical coordinates, $K(s)$ is the focusing function. For the horizontal closed orbit error, $\Delta B(s)$ arises from the vertical dipole field error due to quadrupole horizontal misalignment and dipole field errors. For the vertical closed orbit error, $\Delta B(s)$ arises from the horizontal dipole field error due to quadrupole vertical misalignments and dipole rotations.

2.1 Orbit kick due to a quadrupole

When a single quadrupole is shifted away from the central closed orbit by Δ_q, the angular kick due to the quadrupole is given by $-(y-\Delta_q)/f_q$ in the thin lense approximation, where f_q is the the focal length of the quadrupole and y is the actual closed orbit. For a focusing quadrupole, $f_q > 0$ and similarly $f_q < 0$ for a defocusing quadrupole. Thus the particle closed orbit after the quadrupole is related to the closed orbit before the quadrupole by,

$$\begin{pmatrix} y_a \\ y'_a \\ 1 \end{pmatrix} = \begin{pmatrix} 1 & 0 & 0 \\ -\frac{1}{f_q} & 1 & \frac{\Delta_q}{f_q} \\ 0 & 0 & 1 \end{pmatrix} \begin{pmatrix} y_b \\ y'_b \\ 1 \end{pmatrix}. \tag{2}$$

2.2 Closed Orbit Kick due to a Dipole

When a particle passes through a dipole, the closed orbit is modified by the dipole field error. Using a thin dipole approximation, we obtain then

$$\begin{pmatrix} y_a \\ y'_a \\ 1 \end{pmatrix} = \begin{pmatrix} 1 & 0 & 0 \\ 0 & 1 & \Delta\theta \\ 0 & 0 & 1 \end{pmatrix} \begin{pmatrix} y_b \\ y'_b \\ 1 \end{pmatrix}. \tag{3}$$

where $\Delta\theta$ is the dipole field error.

2.3 The Closed Orbit Error Propagation

The error propagation of the closed orbit is then obtained from multiplying matrices of orbit kicks discussed in previous sections and matrices of appropriate drift spaces. The procedure is equivalent to integrating Eq.(1) along the beam line. This procedure remains valid in the thick lense calculation. Thin lense approximation however simplify the calculation greatly. The final closed orbit distortion can then be expressed in terms of the angular errors of dipoles and quadrupole misalignments of quadrupoles by substituting the quadrupole strengths correspondingly. The actual result of these calculations[2] for RHIC will be discussed in the next section.

3. Closed Orbit Kicks in a RHIC Insertion

Table 1 lists the sensitivity coefficients for the horizontal closed orbit error at Q5, Q3, Q2, Q1 and IP as a function of the error fields discussed in section 2. As an example, table 1 gives the closed orbit deviations at Q3 and IP (for β^*=2m) as,

$$x_3 = -7\ x_9 - 123\ x'_9 + 2.72\ \Delta_8 - 12.5\ \Delta_7 + 3.5\ \frac{\Delta\theta}{\theta} +$$

$$+4.26\ \Delta_6 + 1.1\ \frac{\Delta\theta_s}{\theta_s} - 8.17\ \Delta_5 + 5.76\ \Delta_4$$

0-7803-0135-8/91$01.00 ©IEEE

and

$$x_{IP} = 1.3\ x_9 + 18.1\ x_9' - 0.97\ \Delta_8 + 3.32\ \Delta_7 - 0.85\ \frac{\Delta\theta}{\theta}$$
$$-0.85\ \Delta_6 - 0.18\ \frac{\Delta\theta_s}{\theta_s} + 1.14\ \Delta_5 - 0.53\ \Delta_4 - 2.62\ \Delta_3$$
$$+3.18\ \Delta_2 - 2.37\ \Delta_1 + 0.30\ \frac{\Delta\theta_{c2}}{\theta_{c2}} + 0.21\ \frac{\Delta\theta_{c1}}{\theta_{c1}}$$

We observe clearly that the closed orbit, x_3, at Q3 (similarly at Q2 and Q1) is very sensitive to x_9'. A 0.1 mrad error in x_9' can give rise to 12 mm error at Q3 location by assuming a perfect machine elsewhere. This sensitivity is due to betatron phase advance between Q3 and Q9 and a large betatron function at Q3 position. At the same time, x_3 is also sensitive to quadrupole misalignment at Q7. A 0.25 mm alignment in Q7, Q6, Q5 and Q4 can cause 3 mm rms closed orbit error at Q3. Similarly, the closed orbit at IP is sensitive to Q1–Q3 quadrupole alignment.

Table 1: Sensitivity Coefficients of the horizontal Closed Orbit Displacement. Here $\delta\theta = \Delta\theta/\theta$ represents percentage dipole field error.

β^*=.5m	x_5	x_3	x_2	x_1	x_{IP}	x'_{IP}
x_9	-1	-15.5	-8.6	-10.3	3.1	0.5
x_9'	-11.2	-246	-137	-164.	46.4	8.6
Δ_8	1.06	8.57	4.71	5.62	-1.89	-0.3
Δ_7	-3.37	-34.2	-18.8	-22.5	7.19	1.2
$\delta\theta$	.79	8.68	4.8	5.74	-1.8	-0.31
Δ_6	.27	3.85	2.14	2.56	-0.77	-0.13
$\delta\theta_s$	.07	1.63	0.91	1.1	-0.31	-0.06
Δ_5		0	0	0	0	0
Δ_4		5.3	3.03	3.72	-0.65	-0.18
Δ_3			-0.59	-1.23	-2.57	-0.05
Δ_2				0.6	3.16	0.1
Δ_1					-2.42	-0.1
$\delta\theta_{c2}$					0.30	0.02
$\delta\theta_{c1}$					0.21	0.01
β^*=2m	x_5	x_3	x_2	x_1	x_{IP}	x'_{IP}
x_9	-0.8	-7	-3.8	-4.6	1.3	0.2
x_9'	-2.5	-123.	-69.1	-83.5	18.1	4.1
Δ_8	1.46	2.72	1.4	1.58	-0.97	-0.1
Δ_7	-3.91	-12.5	-6.7	-7.8	3.32	0.45
$\delta\theta$	0.9	3.5	1.88	2.21	-0.85	-0.12
Δ_6	0.64	4.26	2.34	2.78	-0.85	-0.15
$\delta\theta_s$	0.07	1.1	0.61	0.73	-0.18	-0.04
Δ_5		-8.17	-4.59	-5.56	1.14	0.27
Δ_4		5.76	3.3	4.05	-0.53	-0.19
Δ_3			-0.59	-1.23	-2.62	-0.06
Δ_2				0.6	3.18	0.1
Δ_1					-2.37	-0.1
$\delta\theta_{c2}$					0.30	0.02
$\Delta\theta_{c1}$					0.21	0.01

The table also gives us a guide line for the stability requirement in the power supply. As an example, we find

$$x_{IP} = -0.85\ \frac{\Delta\theta}{\theta} - 0.18\ \frac{\Delta\theta_s}{\theta_s} + 0.30\ \frac{\Delta\theta_{c2}}{\theta_{c2}} + 0.21\ \frac{\Delta\theta_{c1}}{\theta_{c1}}$$

from table 1 at β^*=2m. A power supply ripple will affect $\Delta\theta/\theta$ for all dipoles coherently. At $\Delta\theta/\theta \simeq 10^{-4}$, we expect the orbit will be shifted by 0.05 mm in comparison with the $\sigma_{\text{beam size}} \simeq 0.3$ mm for heavy ion beam at 100 GeV/u. The effect will be very harmful to the beam life time due to the presence of beam–beam interaction. It is therefore important to achieve the power supply ripple less than $\frac{\Delta\theta}{\theta} \leq 10^{-5}$. At $\beta^* = 0.5$ m, table 1 gives

$$x_{IP} = -1.8\ \frac{\Delta\theta}{\theta} - 0.31\ \frac{\Delta\theta_x}{\theta_s} + 0.30\ \frac{\Delta\theta_{c2}}{\theta_{c2}} + 0.21\ \frac{\Delta\theta_{c1}}{\theta_{c1}}$$

At $\Delta\theta/\theta \simeq 10^{-5}$ ripple will give $\Delta x_{IP} \simeq 0.02$ mm in comparison with the proton beam size $\sigma = 0.08$ mm at 250 GeV/c. Thus the power supply stability is especially important to the proton collision mode.

Table 2: Sensitivity Coefficients of the Vertical Closed Orbit. Here ϕ is the dipole rotation angle.

β^*=.5m	z_5	z_3	z_2	z_1	z_{IP}	z'_{IP}
z_9	-1.4	3.6	6.7	4.2	-2.5	-0.3
z_9'	18	-79.3	-141.	-87.9	60.5	6
Δ_8	-4.5	17.08	30.71	19.11	-12.5	-1.28
Δ_7	2.44	-8.78	-15.8	-9.86	6.36	0.66
φ	.62	-1.94	-3.53	-2.2	1.35	0.14
Δ_6	-.27	0.55	1.03	0.65	-0.31	-0.04
φ_s	.07	0.02	0.01	0	-0.08	0
Δ_5		0	0	0	0	0
Δ_4		-5.3	-9.27	-5.7	4.49	0.41
Δ_3			0.59	0.53	1.4	0.04
Δ_2				-0.6	-6.05	-0.22
Δ_1					2.42	0.1
φ_{c2}					0.30	0.02
φ_{c1}					0.21	0.01
β^*=2m	z_5	z_3	z_2	z_1	z_{IP}	z'_{IP}
z_9	-1.1	2.5	4.7	3	-1.5	-0.2
z_9'	9.4	-40.8	-73.1	-45.5	31.8	3.1
Δ_8	-3.21	9.31	17.05	10.72	-6.34	-0.69
Δ_7	1.77	-4.52	-8.36	-5.27	2.91	0.33
φ	0.51	-0.95	-1.8	-1.15	0.5	0.07
Δ_6	-0.64	0.42	0.94	0.64	0.14	-0.02
φ_s	0.07	0.11	0.15	0.09	-0.17	-0.01
Δ_5		2.07	3.54	2.16	-2.02	-0.17
Δ_4		-5.76	-10.0	-6.2	5.04	0.45
Δ_3			0.59	0.53	1.39	0.03
Δ_2				-0.6	-6.01	-0.22
Δ_1					2.37	0.1
φ_{c2}					0.30	0.02
φ_{c1}					0.21	0.01

Table 2 lists the sensitivity table for the vertical closed orbit by integrating Eq. (1) along the insertion, where the quadrupole vertical misalignment is given by $\Delta_1, \ldots, \Delta_8$ and the dipole rotation is given by φ, φ_s, φ_{c2} and φ_{c1} for the corresponding dipoles B, BSI, BC2 and BC1 respectively.

Similar to that of the horizontal motion, the quadrupole alignment of Q1–Q3 is important to the proper collision at

IP. Power supply ripple is also critical for the operation at $\beta^* \leq 2$ m.

4. Closed Orbit of the Accelerator

We have calculated the closed orbit error propagation from the begining of the insertion to the interaction point, i.e.

$$\begin{pmatrix} y_{IP} \\ y'_{IP} \\ 1 \end{pmatrix} = \begin{pmatrix} a_{11} & a_{12} & a_{13} \\ a_{21} & a_{22} & a_{23} \\ 0 & 0 & 1 \end{pmatrix} \begin{pmatrix} y_9 \\ y'_9 \\ 1 \end{pmatrix}, \tag{4}$$

where the matrix elements a_{ij} may be obtained directly form Tables 1 and 2. For example, $a_{11} = 3.1, a_{12} = 46.4$ and $a_{13} = -1.89\Delta_8 + 7.19\Delta_7 - 1.8\delta\theta + \cdots$ etc. for the horizontal closed orbit propagation at $\beta^* = 0.5$ m. To obtain a proper closed orbit of the entire circular accelerator, we shall assume that the orbit is propagated through the rest of the machine, i.e.

$$\begin{pmatrix} y_9 \\ y'_9 \\ 1 \end{pmatrix} = \begin{pmatrix} M_{11} & M_{12} & M_{13} \\ M_{21} & M_{22} & M_{23} \\ 0 & 0 & 1 \end{pmatrix} \begin{pmatrix} \tilde{y}_{IP} \\ \tilde{y}'_{IP} \\ 1 \end{pmatrix}. \tag{5}$$

where 2×2 matrix corresponds to the propagation of betatron motion from the IP through the rest of the accelerator to the end of Q9. The matrix elements M_{13}, M_{23} are related the orbit kicks associated with the rest of the accelerator. The total closed orbit is then obtained by multiplying matrices of Eqs. (4) and (5) with the following constraints,

$$\tilde{y}_{IP} = y_{IP}; \quad \tilde{y}'_{IP} = y'_{IP}. \tag{6}$$

The 2×2 matrix of the final product corresponds to the one turn betatron transfer map. They are given by

$$a_{11}M_{11} + a_{12}M_{21} = \cos 2\pi\nu + \alpha^* \sin 2\pi\nu,$$

$$a_{11}M_{12} + a_{12}M_{22} = \beta^* \sin 2\pi\nu,$$

$$a_{21}M_{11} + a_{22}M_{21} = -\gamma^* \sin 2\pi\nu,$$

$$a_{21}M_{12} + a_{22}M_{22} = \cos 2\pi\nu - \alpha^* \sin 2\pi\nu,$$

where ν is the betatron tune for either horizontal or vertical betatron motion, α^*, β^* and γ^* are the Courant-Snyder parametrization of the betatron functions at IP. Normally $\alpha^* = 0$ and $\gamma^* = 1/\beta^*$. Solving the closed orbit condition of Eq.(6), we obtain then

$$y_{IP} = \frac{1}{2\sin\pi\nu}\{(a_{11}M_{13} + a_{12}M_{23} + a_{13})\sin\pi\nu$$
$$+ \beta^*(a_{21}M_{13} + a_{22}M_{23} + a_{23})\cos\pi\nu\}. \tag{7}$$

$$y'_{IP} = \frac{1}{2\sin\pi\nu}\{-\frac{1}{\beta^*}(a_{11}M_{13} + a_{12}M_{23} + a_{13})\cos\pi\nu$$
$$+ (a_{21}M_{13} + a_{22}M_{23} + a_{23})\sin\pi\nu\}. \tag{8}$$

Note here that the orbit error is enhanced by the nearness of the betatron tune to an integer. The sensitivity factor is however still proportional to the tables 1 and 2 through a_{13} and a_{23} coefficients in Eqs. (7) and (8).

5. Conclusion and Discussion

The closed orbit analysis for the RHIC insertion is analyzed in an analytic model in terms of the quadrupole alignment errors and the dipole errors. We calculate the sensitivity coefficients for various β^* values. The closed orbit error becomes large at the high-β quadrupoles, Q1-Q3. To minimize these errors, one should properly align the quadrupoles in the insertion. One should also measure x_9, x'_9, z_9 and z'_9 so that a proper orbit correction scheme for the insertion can be established due to the fact that the closed orbit is sensitively dependent on the parameters x'_9 and z'_9 (see Tables 1 and 2).

Using the table, we can also set the tolerance on the power supply ripple. At low β^* value, the power supply ripple of 10^{-5} is critical to obtain a proper beam-beam collision.

Finally the ground motion due to the high tide, local traffic, etc. will shift quadrupole alignment. A shift of 10 μ in Q1-Q3 can also cause beam movement at the IP by 0.01 mm, which will affect the performance. Fortunately, the ground motions which does not change the relative motion of the accelerator component do not affect the luminosity. The random noise is however normally small, $\simeq 1$ μ. Thus the effect should not be important. Realistic measurement of the effect in RHIC tunnel should be confirmed.

The method described in this paper is useful in evaluating the effect of few important magnetic elements on the closed orbit distortion. Another possible application is analyzing the orbit distortion of a beam tranfer line.

---

* Work performed under the auspices of the U.S. Department of Energy.

† On leave of absence from Brookhaven National Laboratory

Reference

1. E.D. Courant and H.S. Snyder, Ann. of Phys. 3, 1 (1958)

2. S.Y. Lee and S. Tepikian, AD/RHIC-64, Feb. 1990.